Computers and Concrete, *Vol. 24, No. 2 (2019) 103-115*
DOI: https://doi.org/10.12989/cac.2019.24.2.103

Analytical, experimental and numerical study of timber-concrete composite beams for bridges

Julio C. Molina[*1], Carlito Calil Junior[2], Diego R. de Oliveira[3] and Nádia B. Gomes[1]

[1]*Mechanical Engineering Department, University of São Paulo State - UNESP, 333 Ariberto Pereira da Cunha, Pedregulho, Guaratinguetá-SP, 12516-410, Brazil*
[2]*Department of Structural Engineering, São Carlos School of Engineering of the University of São Paulo, 400 Trabalhador São-carlense Street, Downtown, São Carlos - SP, 13566-590, Brazil*
[3]*Wood Science and Engineering Department, Oregon State University, 119 Richardson Hall 97331 - Corvallis, USA*

(Received October 17, 2017, Revised March 8, 2019, Accepted May 3, 2019)

Abstract. In this study, the strength and stiffness (EI) of wood-concrete composite beams for bridges with T-shaped cross section were evaluated. Two types of connectors were used: connectors bonded with epoxy adhesive and connectors attached to the wood just by pre-drilling (without adhesive). The connectors consisted of common steel bars with a diameter of 12.5 mm. Initially, the strength and stiffness (EI) of the beams were analyzed by bending tests with the load applied at the third point of the beam. Subsequently, the composite beams were evaluated by numerical simulation using ANSYS software with focus on the connection system. To make the composite beams, Eucalyptus citriodora wood and medium strength concrete were used. The slip modulus K and the ultimate strength values of each type of connector were obtained by direct shear tests performed on composite specimens. The results showed that the connector glued with epoxy adhesive resulted in better strength and stiffness (EI) for the composite beams when compared to the connector fixed by pre-drilling. The differences observed were up to 10%. The strength and stiffness (EI) values obtained analytically by Möhler' model were lower than the values obtained experimentally from the bending tests, and the differences were up to 25%. The numerical simulations allowed, with reasonable approximation, the evaluation of stress distributions in the composite beams tested experimentally.

Keywords: timber-concrete; composite beams; stiffness EI; strength; numerical simulation; steel bar connector; analytical Möhler model

1. Introduction

Brazil has a large number of wooden bridges. These bridges have an efficient structural performance and are composed of main elements: beams (timber logs or sawn timber) and decks (sawn timber boards), and by secondary elements: railing and wheel guards. The beam bridges are the most common type of wooden bridge and the beams are used in the form of single span. The decks of sawn timber boards, although widely used due to its low cost, present various problems such as the loosening of the boards because of the passage of vehicles over the bridge, especially if the boards are fixed with nails. Moreover, in this type of deck the use of asphalt coating is not common because of the large displacements presented by this system. Fig. 1 illustrates a typical section of a wooden bridge with sawn timber plank decking used in Brazil.

An efficient alternative for wood bridges in Brazil consists of the use in wood-concrete composite decks. On the composite deck, an armed concrete slab is connected to the timber beams so that both materials, concrete and wood, work together. The combined actions in the timber (tension) and in the concrete (compression) under bending are

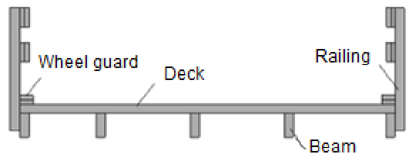

Fig. 1 Section of a wooden bridge with deck of sawn boards. Source: Molina (2008)

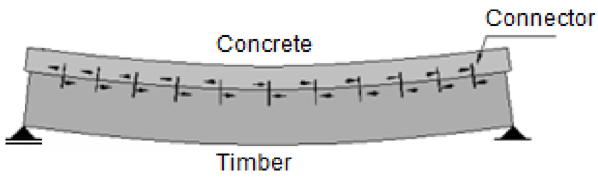

Fig. 2 Shear connectors in a timber-concrete composite beam. Source: Molina (2008)

obtained using shear connectors. These connectors are arranged along the interface of the materials, and they transmit the longitudinal shear forces and prevent the vertical separation of the concrete slab from the timber beams, Fig. 2.

There are several types of connectors used in timber-concrete composite structures and the main features that allow comparisons between them are the ultimate strength, the sliding module *K*, and the final installation cost (Molina 2008).

∗Corresponding author, Ph.D.
E-mail: julio.molina@unesp.br

ISSN: 1598-8198 (Print), 1598-818X (Online)

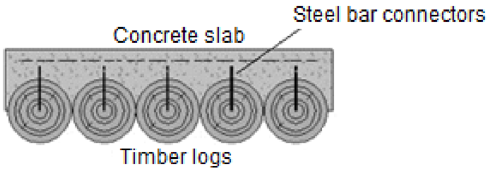

Fig. 3 Economic solution for composite section of wooden bridge. Source: Molina (2008)

Studies and technological innovations have contributed to greater reliability of timber-concrete composite structures (Soriano and Mascia 2009, Tomasi 2010, Miotto and Dias 2011, Yeoh *et al*. 2011, Dias and Jorge 2011, Monteiro *et al*. 2015, Valipour *et al*. 2016, Berardinucci *et al*. 2017).

The connections using steel bars to join two different materials have received the attention of researchers due to the low cost and because of its connections are simple and easy to perform. The connection is characterized by bonding common steel bars in larger diameter holes using structural adhesives. There are no Brazilian technical standards regulating the use of glued steel bars, although they have been used for over twenty years in some Scandinavian countries and in Germany (Pigozzo *et al*. 2017). Currently, the Eurocode 5 standard also does not provide technical rules for the use of steel bars in wood pieces (Maria and Ianakiev 2015). Thus, the bonding of steel bars in wood pieces has been guided based on scientific works developed on this theme.

According to Molina and Calil Junior (2010), a simple and economical solution consists of using steel bar connectors arranged along wood logs, fixed only by pre-drilling on smaller diameter wood. In this case, an armed concrete slab must be built on the wood logs, which are positioned side by side, as shown schematically in Fig. 3. In Australia, Yttrup and Nolan (2001) also adopted this solution.

The composite structures consist of a solution capable of prolonging the useful life of wooden bridges, protecting them from environmental actions and from the wear caused by vehicular traffic. The composite system of timber and concrete allows spans up to twelve meters long, thus meeting the need of the vast majority of Brazilian roads. By using a connection system between the timber and the concrete, a superstructure with more rigid sections and with greater load capacity is obtained. Moreover, if the use of concrete slabs represents an increase in the weight of the existing structure, on the other hand it contributes to the reduction of the dynamic effect resulting from the passage of the vehicles over the bridge. Therefore, in this work the main objective was to evaluate (analytical, experimental and numerical) of timber-concrete composite beams with two types of connections performed by common steel bar segments: glued to a larger diameter wood and fixed to a smaller diameter wood (without the use of adhesive). The analytical study was based on Möhler' model (Molina *et al*. 2015, Molina *et al*. 2006), which is available in Eurocode 5 (2004) standard. Subsequently, experimental bending tests in composite beams were performed to determine the experimental values of stiffness (EI) and ultimate strength for comparison with the analytical results. Finally, the distribution of stresses in the composite beams by numerical simulations using ANSYS software was evaluated and the failure modes of the beams were identified.

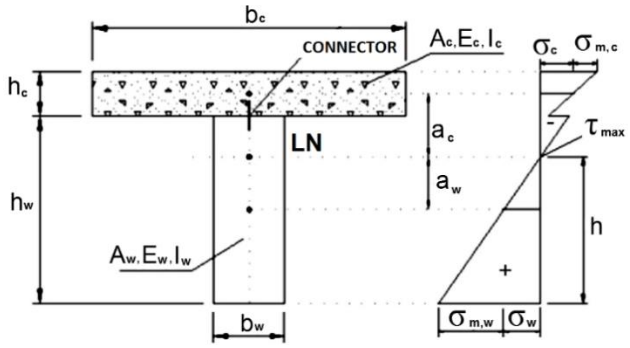

Fig. 4 Stresses in the composite T section. Source: Molina (2008)

2. Calculation of the timber-concrete composite system

The Möhler analytical model considers an equivalent T-beam formed by an armed concrete slab attached to a timber beam by a metallic connection system according to the scheme shown in Fig. 4.

In this model, with the slip modulus (K) of the connector, which is defined experimentally as the angular coefficient of the load versus slip curve, defines the inertia reduction factor of the set in accordance with Eqs. (1) and (2).

$$\gamma_w = 1 \tag{1}$$

$$\gamma_c = \left[1 + \frac{\pi^2 \times E_c \times A_c \times s}{K \times L^2}\right]^{-1} \tag{2}$$

Where: γ_c (inertia reduction factor of the concrete slab), γ_w (inertia reduction factor of the wooden piece), E_c (longitudinal modulus of elasticity of the concrete), A_c (cross sectional area of the concrete), s (spacing between connectors) and L (span between supports).

Eurocode 5 (2004) standard presents the Eq. (3) for the analytical determination of the slip modulus K (N/mm) of connections between wood pieces with steel pin connectors, positioned perpendicular to the shear plane considering the pre-drilling of wood.

$$k_{ser} = \rho_k^{1.5} \times \frac{d}{20} \tag{3}$$

Where: d (diameter of the connector, in mm), ρ_k (characteristic density of wood, in kg/m^3).

The ultimate slip modulus is provided by Eq. (4).

$$k_u = \frac{2}{3} \times k_{ser} \tag{4}$$

The distances between the centers of gravity of each element of the section and the neutral axis are provided by Eqs. (5) and (6).

$$a_w = \frac{\gamma_c \times E_c \times A_c \times (h_w + h_c)}{2 \times (\gamma_c \times E_c \times A_c + \gamma_w \times E_w \times A_w} \quad (5)$$

$$a_c = \left[\frac{h_c + h_w}{2}\right] - a_w \quad (6)$$

Where: h_c (height of the concrete slab), h_w (height of the wooden piece), b_c (width of the concrete slab) and b_w (width of the wooden piece).

The moment of inertia of each element of the composite section is obtained by Eqs. (7) and (8)

$$I_c = \frac{b_c \times h_c^3}{12} \quad (7)$$

$$I_c = \frac{b_w \times h_w^3}{12} \quad (8)$$

Where: I_w (moment of inertia of the wooden piece) and I_c (moment of inertia of the concrete piece).

The effective stiffness in the longitudinal direction of the composite beam results in Eq. (9)

$$\begin{aligned}(EI)_{ef} &= E_c \times I_c + \gamma_c \times E_c \times A_c \times a_c^2 + E_w \times I_w \\ &+ \gamma_w \times E_w \times A_w \times a_w^2\end{aligned} \quad (9)$$

The normal stresses at the ends of the concrete and wood elements are respectively given by Eqs. (10) and (11)

$$\sigma_c = \gamma_c \times E_c \times A_c \times a_c \times \frac{M}{(EI)_{ef}} + 0.5 \times E_c \times h_c \times \frac{M}{(EI)_{ef}} \quad (10)$$

$$\sigma_w = \gamma_w \times E_w \times A_w \times a_w \times \frac{M}{(EI)_{ef}} + 0.5 \times E_w \times h_w \times \frac{M}{(EI)_{ef}} \quad (11)$$

Where: M (bending moment in the section considered)

The maximum shear stress occurs in the neutral line (LN) of the T cross section and is given by Eq. (12) while the shear force on the connectors is given by Eq. (13)

$$T_w = T_{w,\max} = 0.5 \times E_c \times h^2 \times \frac{V}{(EI)_{ef}} \quad (12)$$

$$F = \gamma_c \times E_c \times A_c \times a_c \times s \times \frac{V}{(EI)_{ef}} \quad (13)$$

Where: V=maximum shear force in the section considered.

According to ABNT NBR 6118 (2014) standard, the maximum vertical displacement (deflection) for the concrete under bending is given by Eq. (14).

$$u_{q,\lim} \leq \frac{L}{500} \quad (14)$$

Where: $u_{q,lim}$ (limit of deflection for the concrete, measured in mid span, due to the accidental load).

For wood, according to the revised version of standard ABNT NBR 7190 (2013), the maximum deflection due to accidental loads is given by Eq. (15).

$$u_{\lim} \leq \frac{L}{300} \quad (15)$$

Where: u_{lim} (vertical displacement limit for wood, measured in the mid span, due to accidental load).

3. Materials and methods

3.1 Materials

Eucalyptus citriodora wood, without preservative treatment, was used to produce the composite beams, and common steel bars, CA-50 type, with diameter of 12.7 mm for the shear connectors. The steel bar connectors were fixed to the wood using an epoxy adhesive and by pre-drilling smaller diameter holes in the wood. The epoxy adhesive used has the commercial designation “Compound Adesivo” (manufactured by Otto Baumgart-Vedacit). According to the manufacturer, this is a bi-component adhesive (basic composition: epoxy resin+polyamine), cures in 7 days, and is recommended to bond pieces of concrete, wood, and anchors in general. In 24 hours, the compressive strength of the adhesive reaches approximately 100 MPa. A layer of approximately 1 and 2 mm (efficiency: 0.58 m^2/mm) is sufficient to promote the adherence of the adhesive. The concrete used was prepared with trace 1: 2: 2 by weight, with water-cement ratio (*w/c*) of 0.42. Portland cement CP III RS 40, medium sand, gravel 5/8 " and slump of 8 cm were used to obtain a workable concrete for an adequate filling of the wood form that contained the reinforcing steel bars for the concrete. The expected strength of the concrete at 28 days of age was 25 MPa. The rebars used for the concrete represented minimum reinforcement regarding the volume of concrete used (ABNT NBR 6118 standard 2014). The characterization tests for concrete and molding of the test specimens were made in cylindrical specimens measuring 10 cm in diameter and 20 cm in height. These tests were carried out based on the standards ABNT NBR 5738 (2003), ABNT NBR 5739 (2003) and ABNT NBR 8522 (2003). The characterization of wood was based on the Brazilian standard ABNT NBR 7190 (1997). The woods used in the composition of the composite beams had the following apparent densities at 14% moisture content: B1 (1173 kg/m^3), B2 (1045 kg/m^3), B3 (1123 kg/m^3), B4 (937 kg/m^3), B5 (1087 kg/m^3), B6 (1093 kg/m^3), B7 (950 kg/m^3) and B8 (1005 kg/m^3). The beams B1, B5 and B6 had connectors fixed by pre-drilling (without adhesive) and the beams B3, B4 and B7 had connectors bonded by epoxy adhesive. The B2 and B8 beams were used as reference samples, i.e., identical beams with glued connectors (B2) and with connectors fixed by pre-drilling (B8). Similarly, the SP1, SP5 and SP6 specimens were made with connectors fixed by pre-drilling and the SP3, SP4 and SP7 specimens had glued connectors. The SP2 and SP8 specimens were used as reference samples.

3.2 Equipments

A reaction frame with a hydraulic cylinder of 480 kN was used to conduct the bending tests on the composite beams (Fig. 7(a)). The deflection at the mid span of the beams was measurement using mechanical displacement

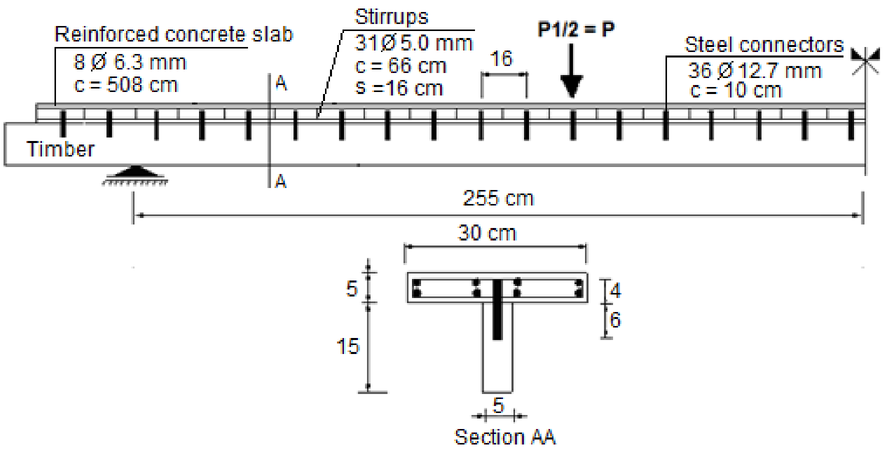

Fig. 5 Symmetrical half of the composite beam with load applied on the thirds of the span

transducers (LVDT) with sensitivity of 0.01 mm and maximum range of 100 mm (Figs. 6 and 7(a)). To measure the displacements on the supports of the beams, during the bending tests, comparator watches with sensitivity of 0.01 mm and maximum range of 50 mm was used (Fig. 7(b)). The loads on the shear test specimens were controlled by a load cell of 250 kN capacity (Fig. 10(a)). For the direct shear test of the specimens, the displacements between the wood and concrete materials were measured by two displacement transducers, type DT 100 A (ER4300016 and ER4300018), with a maximum range of 100 mm, positioned on the opposite faces of the specimens (Fig. 10(a), and instrumentation details in Fig. 8). The data acquisition system (SYSTEM 5000) was set up to read the signals every second. The setup schemes for the composite specimens and beams are shown in Figs. 5 and 8, respectively.

3.3 Fixing of the shear connectors on the wood

The connectors were fixed on the composite beams and specimens with inclination of 90° to the wood fibers, with wood moisture content of 14±1%. For the glued connectors, the diameter used for the holes in the wood was 1.59 cm. This value was obtained by the relation D=1.25.d, according to the recommendations of Buchanan and Moss (1999). For the connectors fixed by pre-drilling (without the use of adhesive), the diameter of holes in the wood was 1.27 cm. The anchorage length (l_a) of the connectors on the wood was 6.0 cm, and the slenderness ratio used, in this case, was λ=4.72 (λ=l_a/d) according to Baimbridge *et al.* (2001). The steel bar connectors after glued were put to rest for seven days to reach the maximum strength of the resin.

3.4 Sample size

Four sample repetitions were considered for the bending and direct shear tests, totalizing 16 tests. Four of these samples were used as twin samples (reference test specimens) to obtain the initial properties of strength and stiffness for each type of connection analyzed in this work.

3.5 Bending test of the composite beams

3.5.1 Configuration

The dimensions of the T cross section for the composite beams were calculated based on the Möhler model. To determine the width of the concrete slab, the shear lag effect was minimized (non-uniformity of the stresses in the width of the concrete slab). The ratio between the heights of the concrete slab and wood piece of the composite beam was 1/3 (expected failure in the concrete slab with subsequently failure under tension in the lower fiber of the wood, according to verifications made using Möhler's model). The length of the composite beams was admitted as representative of a beam of a real size for bridges in Brazil. The size of the span sought to eliminate the portion of shear on the results of the deflection (for L/h>20, where h is the height of the composite beam and L is the span between supports). In the checks based on the Möhler' model, the values of strength and slip modulus K, for the connectors, were obtained from experimental direct shear tests performed on composite specimens. In the composition of the composite beams, sawn wood pieces with rectangular cross sections of 5 cm×15 cm were used (cross section available in local commerce), and a rectangular concrete slab with dimensions of 30 cm×5 cm. The minimum cover for the concrete reinforcement in this case was 10 mm. This value is less than 20 mm as recommended by standard ABNT NBR 6118 (2004) for slabs considering the level of aggressiveness of the environment I. However, this does not invalidate this study which focuses on the strength and stiffness of the connection system used. It was used a span of 5.10 m and each composite beam presented approximately 6 meters long. In each composite beam, 36 shear connectors spaced 16 cm apart were used. Fig. 5 shows the main details of the composite beams.

3.5.2 Application of load in the experimental tests

The bending tests for the experimental determination of the ultimate strength and stiffness $(EI)_{exp}$ of composite beams were conducted by applying forces P1/2 on the thirds of the span (Figs. 5 and 6). The loads on the beams were applied with three load cycles.

The first and the second cycle were applied until 50% ultimate load of the composite beam (determined from the twin sample: B2 and B8, depending on the connector

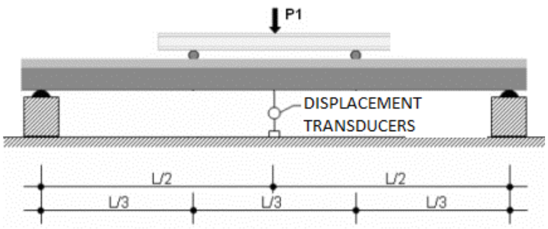

Fig. 6 Layout of the bending test of the composite beams according to Miotto and Dias (2015)

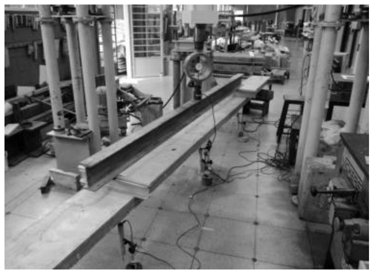

(a) General instrumentation of the beam

(b) Instrumentation of the support areas

Fig. 7 Details of the experimental bending test of composite beams. Source: Molina (2012)

analyzed). The third cycle was progressively applied until the failure of the composite beam by tension of the lower wood fiber in the bottom part of the wooden piece. A mechanical displacement transducer was used to measure the deflections in the mid span of the beams. The value of the experimental stiffness $(EI)_{exp}$ of beams considered a service load P1 that causes a deflection of 1.70 cm (L/300, where L is the span between supports, according to ABNT NBR 7190 2013). The load value P1 was the value admitted for the beams working in the service system. Fig. 7 shows the details of the bending test of the composite beams.

The experimental stiffness values $(EI)_{exp}$ of the composite beams were determined using Eq. (16).

$$(EI)_{\text{exp}} = \frac{P \times a \times 3 \times L^2 - 4 \times a^2}{24 \times \delta} \tag{16}$$

Where: P (value of the load on the third-points of the beam span, P=P1/2), L (span between supports of the beam), δ (deflection related to the load P1), and a (distance from the support to the point that the load is applied, in this case L/3).

3.6 Shear tests of the composite specimens

These tests were to determine the ultimate strength and the slip modulus K of the connection systems used in this study. The length of each rectangular wood piece of the composite specimens was 50 cm, with rectangular cross section of 5 cm×15 cm. In each composite specimen four steel connectors were used, Fig. 8. The reinforcement for the concrete of the composite specimens was equivalent to the concrete of the composite beams, Fig. 9. The shear tests were also performed with three load cycles in this case. The baseline measurement of the displacements considered for the composite specimens was L_0=15 cm. The L_0 value was used to determine the specific deformation (2‰ strain) that causes the failure of the connection system, according to standard ABNT NBR 7190 (1997). Thus, the values of the slip modulus K and strength of the connections were obtained from the points 10% and 40% of the ultimate load, related to the specific deformation of 2‰. Fig. 10 shows the details of the direct shear test performed on the composite specimens, as well as the details of the instrumentation used.

3.7 Calculation of the composite beam T by the Möhler analytical model

The Möhler model was used to determine the analytical stiffness $(EI)_{ef}$ value and also to estimate the limit of load P

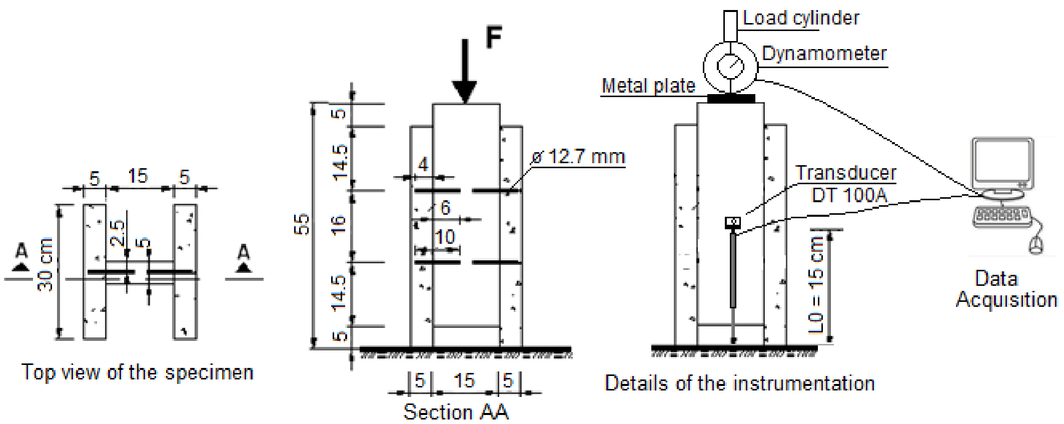

Fig. 8 Configuration of the composite specimens for determination of the slip modulus K and strength for the two types of connectors used in this study. Source: Molina (2012)

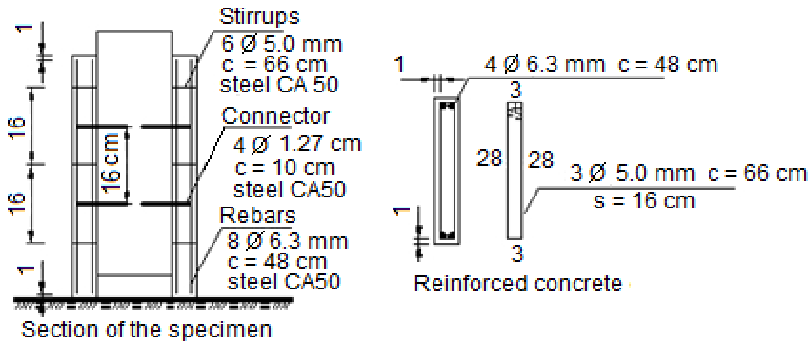

Fig. 9 Details of reinforcing bars of the concrete for the composite specimens. Source: Molina (2012)

(a) Instrumentation of the specimen

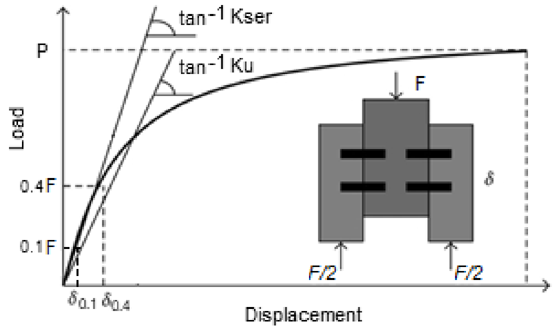

(b) Determination of the slip modules K

Fig. 10 Direct shear test details of the specimens, see Figs. 8 and 9. Source: Molina (2012)

in the bending tests of the composite beams. For service loads (corresponding to L/300 deflection in this work), the determination of the analytical stiffness $(EI)_{ef}$ considered the experimental sliding modulus K_{ser}. Also verified were the composite beams for the maximum loads applied during the bending tests. In this case, the theoretical stiffness values $(EI)_{ef}$ were obtained based on the ultimate sliding modulus k_u, Eq. (4). Thus, for the composite beams the limit values of force P required to cause the failure in the composite section T (concrete slab, steel connection system, or wood piece) were verified. The bending moment and shear force values according to the load P applied on the thirds of the span, in this case, were, M=PL/3 and V=P, respectively, see Eqs. (10)-(13).

3.8 Numerical simulation of the composite beam using the ANSYS software

The numerical simulations were using two tridimensional models with the ANSYS software, version 10.0, which is based on the Finite Element Method (FEM).

The proposed numerical models allowed, in a complementary character, the evaluation of the stress levels in the regions of greatest interest of the composite beams, i.e., concrete, wood and mainly steel connectors.

3.8.1 Solid65 element

Solid65 was used in the discretization of the concrete pieces. The option for this element was due to the simulation possibility of the localized effects, such as the concentration of stresses in the shear connector areas. The solid65 is a hexahedral element, which has eight nodes (each node has three degrees of freedom, i.e., translations along the x, y, and z axes). This element is able to simulate the behavior of the concrete with cracking under tension and crushing under compression, as well as behavior with physical non-linearity, which allows evaluating the plastic deformations.

3.8.2 Link8 element

Link8 was used in the discretization of reinforcing steel bars for the concrete. This element consists of a three-dimensional bar element, which has two nodes, each node with three degrees of freedom (translations along the x, y and z axes), and responds to axial tensile and compressive stresses. The "x" axis of the element is oriented along its length and no bending in the element was considered. However, it is possible to admit the occurrence of plastic deformation for the material in this case.

3.8.3 Solid45 element

This element was used in the discretization of the wood pieces and the steel connectors. The solid45 consists of a hexagonal element with eight nodes, each node has three degrees of freedom (translations along the x, y and z axes), and allows the considering important effects such as plasticity and orthotropic behavior of the materials.

3.8.4 Conta 173 and Targe 170 elements

These two elements were used to represent the existing contacts with possible displacements in the following interfaces: wood-concrete, steel-concrete and steel-wood. These elements are used in three-dimensional analyses, with surface-to-surface contact, which arises from working

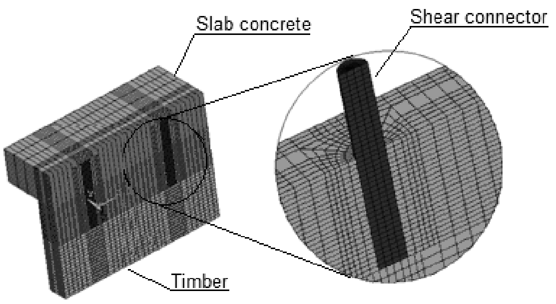

Fig. 11 Refinement of the mesh in the shear connector areas (numerical models)

together with the targe170 element (defined by ANSYS as the target surface) and conta 173 (defined as contact surface). These elements are able to simulate the existence of pressure between the elements, when there is contact, and separation between the same elements when there is no contact. The pair of contacts used also allows considering of the friction between the parts.

3.8.5 Discretization of the meshes and boundary conditions

The meshes of the numerical models were analyzed from different levels of refinement until the results lead to satisfactory responses in terms of displacements and deformations. Fig. 11 shows the details of a central part of the composite beam, which contains the discretization adopted for the shear connector areas. The areas of the shear connectors had a higher level of refinement for evaluating the stress distributions at these locations.

To reduce the processing time of the models, it was chosen to model ¼ of the geometry of the composite beam, considering the conditions of symmetry for the models. Thus, in each model, the applied load intensity was defined by dividing the failure load estimated in the experimental analysis (¼ of structure) by the number of nodes in the region relative to the load application.

This strategy was used to avoid problems of convergence during the numerical processing of the models. It should be noted that in the actual test, to allow applying the load in the thirds of the beams span, two smaller metal beams with I cross section were positioned transversely on the concrete piece (Fig. 7(a)). The point of application of the loads and the measurement of deflection (mid span) in the numerical models were performed in agreement with the experimental bending tests of the composite beams. The numerical models were validated by comparing the behavior of the experimental load versus deflection (mid span) curves (see calibration curves, Fig. 16) based on Fig. 12(a). Subsequently, with the calibrated models, the stiffness $(EI)_{num}$ values were obtained numerically using ANSYS software, considering Eq. (16). The $(EI)_{num}$ values were compared with experimental and analytical results of EI (Table 5). In order to guarantee the stability of the models during the application of the loads, the symmetry conditions and the support nodes were respected, as shown in Fig. 12 (b) and (c).

3.8.6 Constitutive models for the materials

The constitutive model adopted for the concrete under compression was the multilinear type with isotropic hardening, according to Molina (2008). The stress-strain curve used was obtained from experimental tests performed on concrete cylindrical specimens measuring 10 cm×20 cm.

An orthotropic behavior was adopted for the wood, using the resistance criterion of Hill (1950), associated with the isotropic hardening (Dias 2005).

The constitutive model, adopted for wood, simulates an elastic-plastic behavior, through bi-linear curves, depending on the main directions of the material.

For simplicity, the behavior of the wood under tension and compression was the same. In addition, no distinction was made between the radial and tangential directions and the values considered, in this case, corresponded to the perpendicular direction to the wood fibers (radial direction). The wood properties and their relationships were obtained through experimental tests carried out on wood specimens based on standard ABNT NBR 7190 (1997).

For the shear connectors, a bi-linear model with isotropic hardening and the von Mises yield criterion were adopted. The constitutive relation used for the concrete rebars followed the criterion of von Mises with stress-strain curve based on a perfect elastic-plastic model (Molina 2008).

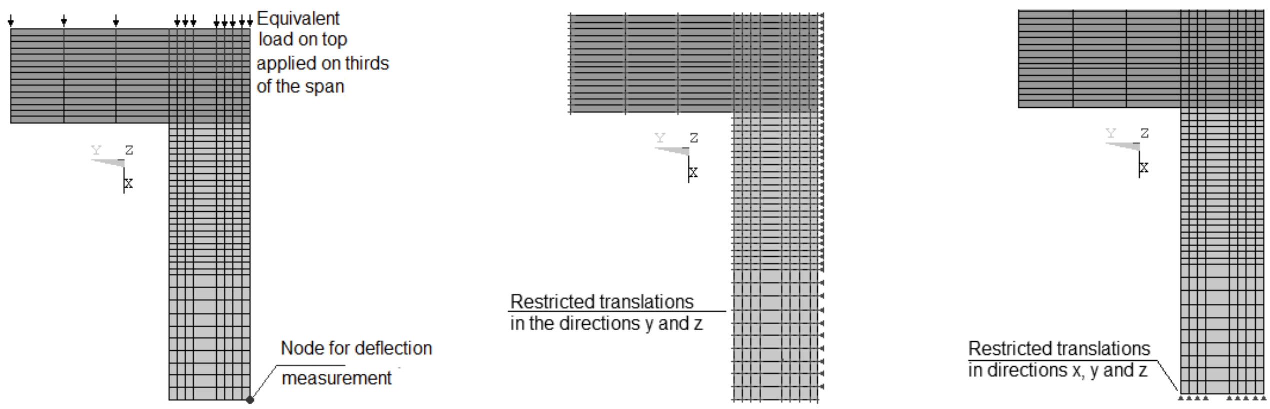

(a) Beam with ¼ of the geometry (b) Symmetry conditions (c) Support conditions

Fig. 12 Boundary conditions and load conditions in the numerical models of the composite beams

Table 1 Characterization of the materials of the composite specimens with four steel bar connectors

Composite specimen	Type of connector	Concrete		Wood			
		$f_{c,m}$ (1) (MPa)	$E_{c,m}$ (2) (MPa)	$f_{c0,m}$ (3) (MPa)	$E_{c0,m}$ (4) (MPa)	ρ_{ap} (5) (kg/m^3)	U (6) (%)
SP1	Pre-drilling	26.02	24157	82.13	20460	1173	14.01
SP2	Pre-drilling	26.02	24157	79.55	18726	1045	14.93
SP3	Glued	26.02	24157	80.00	20586	1123	14.04
SP4	Glued	26.02	24157	81.13	16949	937	14.11
SP5	Pre-drilling	26.02	24157	82.98	20587	1087	14.03
SP6	Pre-drilling	26.02	24157	81.01	19729	1093	14.05
SP7	Glued	26.02	24157	80.25	19726	950	14.40
SP8	Glued	26.02	24157	81.14	20672	1005	14.26

(1) Mean compressive strength of concrete, obtained on the test day (average of 06 repetitions) - according to ABNT NBR 5739 (2003);
(2) Mean compressive modulus of elasticity of concrete, obtained on the test day (average of 06 repetitions) - according to ABNT NBR 8522 (2003);
(3) Mean compressive strength of wood, obtained on the test day (average of 06 repetitions) - according to ABNT NBR 7190 (1997);
(4) Mean compressive modulus of elasticity of wood in direction parallel to the grain (average of 06 repetitions) - according to ABNT NBR 7190 (1997);
(5) Wood apparent density on the test day - according to ABNT NBR 7190 (1997);
(6) Moisture content of wood on the test day - according to ABNT NBR 7190 (1997)

4. Results and discussion

4.1 Experimental direct shear tests of the composite specimens

Table 1 lists the results of the characterization of the materials used in the composite specimens, and Table 2 lists the values of strength and slip modulus K obtained for the connectors of the composite specimens, see Fig. 10.

Figs. 13 and 14 show the behavior of the curves obtained from the shear test of the composite specimens with four vertical connectors for both types of connections glued with epoxy resin and fixed by pre-drilling in the wood (Fig. 10(b)).

The mean values of the slip modulus and the ultimate load of each steel bar connector fixed by pre-drilling in the wood with an average moisture content of 14.26% were K_{ser} =22.16 kN/mm and F_u=27.45 kN. For the glued connector, these values with an average moisture content of 14.20% were, respectively, K_{ser}=27.60 kN/mm and F_u=30.05 kN.

Therefore, in general, it was was observed that the mean strength value of the connector glued with epoxy resin was about 8.65% higher than the strength of the connector fixed by pre-drilling (without resin).

The mean slip modulus K_{ser} of each glued connector was 19.40% higher than the slip modulus obtained for the connector fixed by pre-drilling. The effect of inserting the pin into wood in the connector regions was more pronounced for connectors fixed by pre-drilling (without the use of adhesive). In this case, the steel pin caused greater crushing in the wood, consequently resulting in a lower value for the slip modulus K.

Table 2 Values of load and slip modulus of the composite specimens with four connectors of steel bar

Composite specimen	Type of connector	(1)F_{rup} (kN)	(2)F_u (kN)	F_u/connector (kN)	K_{ser}/connector (kN/mm)	K_u/connector (kN/mm)
SP1	Pre-drilling	119.81	107.01	26.75	21.67	14.45
SP2	Pre-drilling	132.95	111.43	27.86	22.63	15.09
SP3	Glued	152.84	119.83	29.96	27.38	18.25
SP4	Glued	161.19	120.54	30.14	27.60	18.40
SP5	Pre-drilling	120.01	106.21	26.55	21.40	14.27
SP6	Pre-drilling	135.88	114.55	28.64	22.95	15.30
SP7	Glued	153.80	120.78	30.20	28.22	18.81
SP8	Glued	164.76	119.65	29.91	27.20	18.13

(1) F_{rup}: maximum load applied on the specimen for complete failure;
(2) F_u: ultimate load equivalent to the specific deformation (or strain) ε=‰

Table 3 Characterization of the materials of the composite beams for the bending tests

Composite Beam	Type of connector	Concrete		Wood				
		$f_{c,m}$ (1) (MPa)	$E_{c,m}$ (2) (MPa)	$f_{c0,m}$ (3) (MPa)	$E_{c0,m}$ (4) (MPa)	$E_{M,m}$ (5) (MPa)	ρ_{ap} (6) (kg/m^3)	U (7) (%)
B1	Pre-drilling	26.02	24157	82.13	20460	18604	1173	14.01
B2	Pre-drilling	26.02	24157	79.55	18726	17027	1045	14.93
B3	Glued	26.02	24157	80.00	20586	19465	1123	14.04
B4	Glued	26.02	24157	81.13	16949	15411	937	14.11
B5	Pre-drilling	26.02	24157	82.98	20587	19885	1087	14.03
B6	Pre-drilling	26.02	24157	81.01	19729	17939	1093	14.05
B7	Glued	26.02	24157	80.25	19726	14972	950	14.40
B8	Glued	26.02	24157	81.14	20672	19682	1005	14.26

(1) Mean compressive strength of concrete, obtained on the test day (average of 06 repetitions) - according to ABNT NBR 5739 (2003);
(2) Mean compressive modulus of elasticity of concrete, obtained on the test day (average of 06 repetitions) - according to ABNT NBR 8522 (2003);
(3) Mean compressive strength of wood, obtained on the test day (average of 06 repetitions) - according to ABNT NBR 7190 (1997);
(4) Mean compressive modulus of elasticity of wood in parallel direction to the grain (average of 06 repetitions) - according to ABNT NBR 7190 (1997);
(5) Mean compressive modulus of elasticity of the wood in bending (average of 06 repetitions) - according to ABNT NBR 7190 (1997);
(6) Apparent density of wood on the test day - according to ABNT NBR 7190 (1997);
(7) Moisture content of wood on the test day - according to ABNT NBR 7190 (1997)

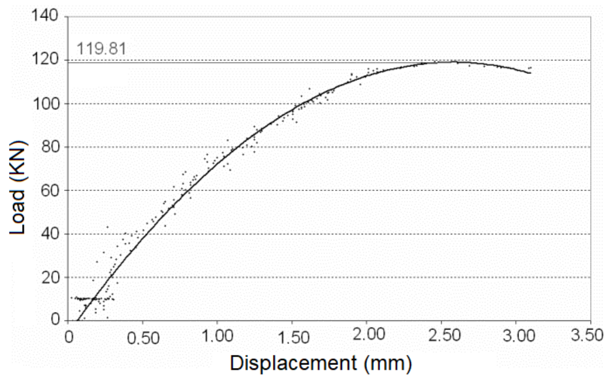

(a) Load (F_{rup}) required for the complete failure of the composite specimen SP1

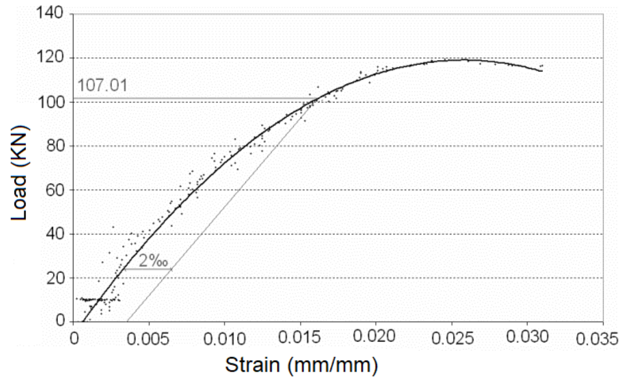

(b) Load (F_u) that causes the deformation of 2‰ on the connection of specimen SP1

Fig. 13 Behavior of the composite specimen SP1 with 4 connectors fixed by pre-drilling (without resin)

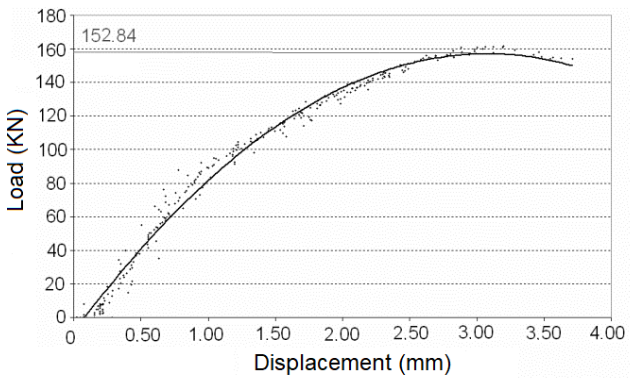

(a) Load (F_{rup}) required for the complete failure of composite specimen SP3

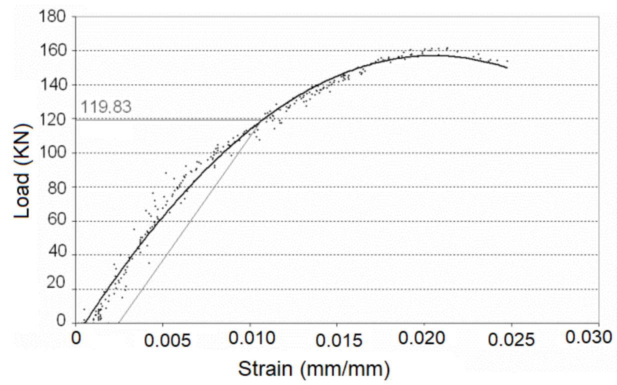

(b) Load (F_u) that causes the deformation of 2‰ on the connection of specimen SP3

Fig. 14 Behavior of the composite specimen SP3 with 4 glued connectors

On the other hand, for the glued connectors, the glue line, which has compressive strength of approximately 100 MPa, contributed to the increase in stiffness of the connection system.

4.2 Experimental bending tests of the composite beams

Table 3 lists the results of the characterization of the wood and concrete used in the composite beams with two types of connectors.

Table 4 shows the load of the bending tests obtained for deflection of 1.70 cm (L/300) in the mid span of the composite beams.

The experimental stiffness $(EI)_{exp}$ values obtained according to Eq. (16), the analytical values obtained by Möhler model according to Eq. (9), as well as the numerical values obtained by numerical simulation in ANSYS software described in item 4.3 are listed in Table 5.

The values presented in this case considered the beams with glued connectors (B3, B4, B7 and B8) and the beams with connectors fixed by pre-drilling without resin (B1, B2, B5 and B6).

The mean value of the experimental stiffness EI obtained for the composite beams with connectors fixed by pre-drilling was 25.59% higher than the theoretical value calculated by the Möhler model.

For the beams with glued connectors, the mean value of the experimental stiffness was 23.09% higher than the analytical value obtained by the Möhler model. The numerical stiffness values agreed with the analytical and experimental values of (EI).

Table 4 Load values in the bending tests to cause a deflection of 1.70 cm (L/300)

Beams with connectors fixed by pre-drilling		Beams with connectors glued with epoxy resin	
Beam	Load (kN)	Beam	Load (kN)
B1	5.62	B3	6.06
B2	4.79	B4	5.10
B5	5.89	B7	5.74
B6	4.94	B8	6.62

Table 5 Mean stiffness EI values (kN.cm^2) for the composite beams considering deflection L/300

Beams with connectors fixed by pre-drilling			Beams with glued connectors		
Beams B1, B2, B5 and B6			Beams B3, B4, B7 and B8		
$(EI)_{ef}$	$(EI)_{\mathrm{num}}$	$(EI)_{exp}$	$(EI)_{ef}$	$(EI)_{\mathrm{num}}$	$(EI)_{exp}$
10,715,94	13,408,12	14,401,83	11,885,50	14,828,12	15,454,27
9.40	5.81	3.33	7.34	9.04	5.00

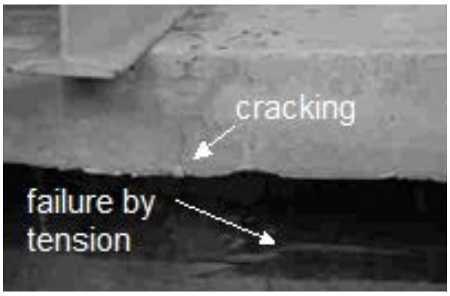

(a) Cracking of concrete slab and failure on the wood fiber (by tension)

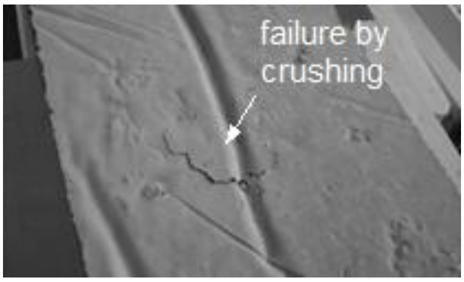

(b) Crushing at the upper end of concrete slab (by compression) in the mid span

Fig. 15 Failure modes obtained in the bending tests of the composite beams with glued connectors

Table 6 Ultimate load (P1) obtained for the composite beams in the experimental bending tests

Beams with connector fixed by pre-drilling		Beams with connector glued with epoxy resin	
Beam	P1 (kN)	Beam	P1 (kN)
B1	59.56	B3	61.98
B2	58.20	B4	60.76
B5	59.89	B7	60.82
B6	58.75	B8	62.04
Mean value	59.10	Mean value	61.40

On the other hand, the numerical results were smaller than the experimental results obtained by the bending tests and larger than the analytical results obtained by the Möhler model for the two types of connectors that were analyzed.

The differences between the numerical and experimental stiffness EI values were 6.9% for the connectors fixed by pre-drilling and 4.05% for the glued connectors.

4.3 Failure modes of the composite beams

The experimental failure load values P1 (see details of the bending test in Fig. 6) obtained for each composite beam in the bending tests are in Table 6. Fig 15 shows the main failure modes observed in the experimental bending tests with composite beams for the two types of connectors analyzed. The main failure modes obtained experimentally for the composite beams under bending tests for the two types of connectors analyzed agreed with those estimated by the Möhler analytical model. The failure on the concrete slab (compression) and on the lower fiber of the wood piece (tension) occurred for the load values 14.44 KN and 25.14 KN, respectively, in the case of beams with connectors

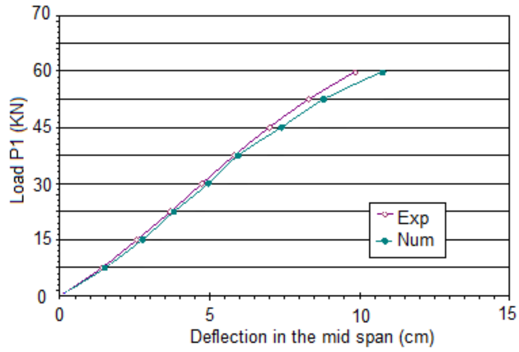

(a) Load versus deflection curve for composite beam B1 (with connectors fixed by pre-drilling)

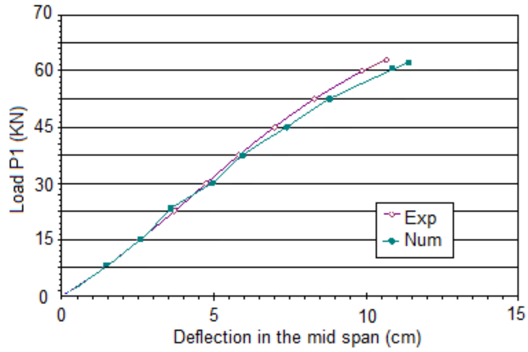

(b) Load versus deflection curve for composite beam B3 (with connectors glued with resin)

Fig. 16 Validation of numerical models with the experimental bending tests

fixed by pre-drilling of wood.

For the beams with glued connectors the load values estimated by the Möhler model were, respectively, 15.23 KN and 25.80 kN.

The Möhler model is a linear model. Thus, in the evaluation of the composite beams, under bending, this theoretical model guarantees a good approximation, mainly when values of service loads are applied on the beams. In this case, the damage on the wood (embedment) and on the concrete (cracking), at the connector regions, occur due to the concentration of stresses, which are generally larger when compared to the stresses from the other regions of the composite beam (see Fig. 17). It can be said that the failures of the materials (wood and concrete), at the connector regions, can be reached before the failure of the other parts of the composite element. These damages (embedment and cracking), located at the connector regions, are not considered by the Möhler model, which considers only the values of the sliding modulus, K_{ser} and K_u, relative to the connector used. The effect of stresses concentration, at the connector regions, becomes more influential when ultimate load values are applied to the beams. Therefore, greater damage at the connector regions, due to the concentration of stresses, result in higher deflection values at the middle span of the beams and, consequently, in larger differences between the theoretical and experimental values of (EI). In view of the fact that the thicknesses of the glue lines used in the glued connector holes helped to increase the strength for the embedment of the steel bar on the wood, it was also

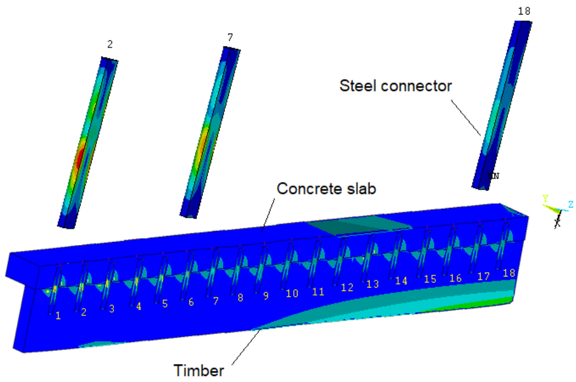

(a) Distribution of stresses in the composite beam (1/4 geometry)

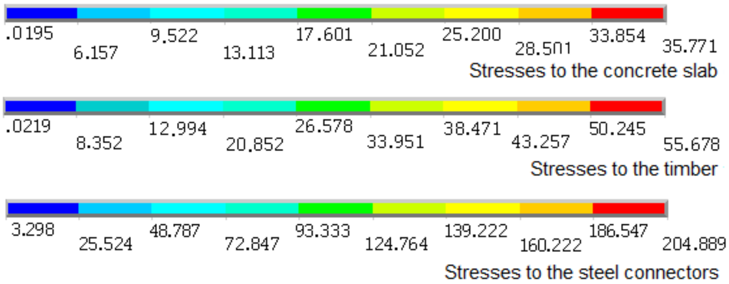

(b) Stress values for the composite beam B1 with connectors fixed by pre-drilling

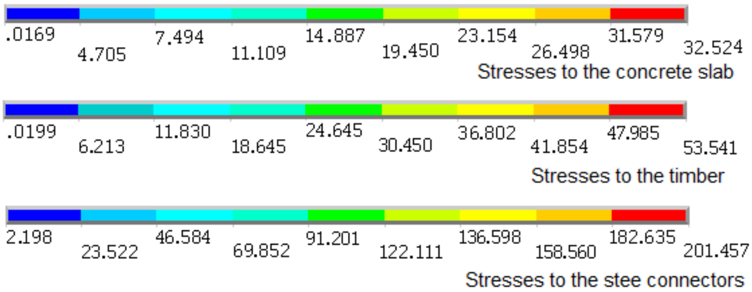

(c) Stress values for the composite beam B3 with connectors glued with resin

Fig. 17 Numerical values of stresses (MPa) for the composite beams obtained using ANSYS software for the ultimate loads P1 applied in the experimental bending tests

observed that this mechanism allowed a better distribution of the stresses in the area of the glued connectors. Thus, for the composite beams with glued connectors, which presented more rigid sections, a greater load was required to promote the same deflection value at the mid span (see Table 4).

4.4 Numerical simulations

Fig. 16 shows the load-deflection curves obtained with the experimental tests of the composite beams, as well as with the numerical simulations to validate the numerical results.

Considering the load values given in Table 6, the error obtained in the calibration between numerical and experimental results (Fig. 16) was up to 7% for the composite beams with glued connectors and up to 10% for the beams with connectors fixed by pre-drilling. However, despite the differences, the numerical and experimental curves presented similar order of magnitude and configuration.

Fig. 17 shows the stress values for the numerical models. Based on the numerical simulations, it was possible to identify the concentration of stresses mainly in the connector areas. This behavior was observed regardless of the type of connector used in the composite *T* section.

In addition, the connectors positioned near the supports were requested by higher stress values than the connectors positioned at the center region of the beam.

Moreover, the numerical models were able to identify the values of stresses in the regions of interest for each of the materials involved in the composite bond.

In other words, the numerical simulations allowed the analysis of the composite beams not only with respect to the global aspect, from the load versus deflection relation (Fig. 16), but also with respect to the localized aspects such as the verification of the stresses in the connector regions and other components of the models.

Moreover, it can be observed that the models proposed herein were able to simulate the mechanical behavior of the shear connectors not only in the linear elastic phase but also at the beginning of the nonlinear phase that begins with the plastification process of the materials.

5. Conclusions

In general, the composite beams with glued connectors presented higher mean values of stiffness EI and of strength when compared to the composite beams with connectors fixed by pre-drilling (without resin). This fact was confirmed in the three analyses (theoretical, numerical and experimental) performed in this research.

The stiffness (EI) results obtained experimentally through the bending tests were slightly higher than the numerical results, and those, by their turn were higher than the theoretical results for the two types of connectors analyzed.

The Möhler model is a linear model and for this reason, provided a good approximation to the $(EI)_{ef}$ values (when compared with the experimental values of $(EI)_{exp}$) mainly when service load values were applied in the composite beams.

The difference between the mean theoretical stiffness $(EI)_{ef}$ values was 9.8% for the two types of connectors analyzed (with and without resin). On the other hand, the difference between the mean experimental stiffness $(EI)_{exp}$ values was 6.8% and for the mean numerical stiffness $(EI)_{num}$ values the difference was 9.58%.

For the mean theoretical values of ultimate load, the difference between the composite beams with connectors glued and fixed by pre-drilling was 5.2%. The difference between the mean experimental values of ultimate load, obtained from the experimental bending tests was 3.7%.

The analytical failure modes obtained for composite beams with the two types of connections agreed with the failure modes obtained experimentally with the bending tests. For both types of connections analyzed, the failures of the beams under bending occurred firstly on the concrete slab, by compression, followed by tension of the lower fiber of the wood piece.

The numerical simulations allowed, with reasonable approximation, evaluating stress distributions in the composite beams tested experimentally, not only globally but also in the areas of the shear connectors.

The finite element SOLID45 used in the modeling of wood pieces considers only elastic and plastic properties of wood. This element was not very flexible and, in this case, even if the finite element mesh was refined, there was no improvement in the behavior of the load versus deflection curves. The use of other finite elements that consider the damage effects (besides the elastic and plastic properties) for the materials involved in the composite bond may allow to quantify more accurately the behavior of the load versus deflection curve for ultimate load values.

Acknowledgments

The research described in this paper was financially supported by the Sao Paulo State Research Support Foundation (FAPESP) - Process number 2008/06726-5.

References

ABNT NBR 5738 (2003), Concrete. Procedure for Molding and Specimens Cure, Brazilian Association of Technical Standards, Rio de Janeiro, Brazil.

ABNT NBR 5739 (2003), Concrete Compression Tests on Cylindrical Specimens, Brazilian Association of Technical Standards, Rio de Janeiro, Brazil.

ABNT NBR 6118 (2014), Design of Concrete Structures. Procedure, Brazilian Association of Technical Standards, Rio de Janeiro, Brazil.

ABNT NBR 7190 (1997), Design of Timber Structures, Brazilian Association of Technical Standards, Rio de Janeiro, Brazil.

ABNT NBR 7190 (2013), Design of Timber Structures, Revision Version, Brazilian Association of Technical Standards, Rio de Janeiro, Brazil.

ABNT NBR 8522 (2003), Concrete. Determination of Static Modules of Elasticity and of Strain and of the Curve Stress-Strain, Brazilian Association of Technical Standards, Rio de Janeiro, Brazil.

ANSYS Inc. (2004), http://www.ansys.com/products/structures

Baimbridge, R.J., Harvey, K. and Mettem, C.J. (2001), "Fatigue Performance of Structural Timber Connections", *Proceedings of International Associations for Bridge and Structural Engineering Conference*, Lahty, Finland, August.

Berardinucci, B., Nino, S., Gregori, A. and Fragiacomo, M. (2017), "Mechanical behavior of timber-concrete connections with inclined screws", *Int. J. Comput. Meth. Exp. Measur.*, **5**(6), 807-820.

Buchanan, A. and Moss, P. (1999), "Design of epoxied steel rods in glulam timber", *Proceedings of the Pacific Timber Engineering Conference*, Rotorua, New Zealand; March.

Dias, A.M.P.G. (2005), *Mechanical Behaviour of Timber-Concrete Joints*, University of Coimbra, Coimbra, District of Coimbra, Portugal.

Dias, A.M.P.G. and Jorge, L.F.C. (2011), "The effect of ductile connectors on the behaviour of timber-concrete composite beams", *Eng. Struct.*, **33**(11), 3033-3042. https://doi.org/10.1016/j.engstruct.2011.05.014.

Eurocode 5 (2004), Design of Timber Structures. Part 1.1: General Rules and Rules Buildings, European Committee for Standardization, Brussels, Belgium.

Hill, R. (1950), *The Mathematical Theory of Plasticity*, Oxford at the Clarendon Press.

Maria, V.D. and Ianakiev, A. (2015), "Adhesives connections in Timber: A comparison between rough and smooth wood bonding surfaces", *Int. Scholar. Sci. Res. Innov.*, **9**(3), 395-401.

Miotto, J.L. and Dias, A.A. (2011), "Glulam-concrete composites: experimental investigation into the connection system", *Mater. Res. (São Carlos. Impresso)*, **14**(1), 53-59.

Miotto, J.L. and Dias, A.A.C. (2015), "Structural efficiency of full-scale timber-concrete composite beams strengthened with fiberglass reinforced polymer", *Compos. Struct.*, **128**(1), 145-154. https://doi.org/10.1016/j.compstruct.2015.03.054.

Molina, J.C. (2008), "Analysis of the dynamic behavior of the connectors formed by bonded-in steel rods for log-concrete composite deck bridges", PhD. Thesis, São Carlos School of Engineering of the University of São Paulo, São Paulo. (in Portuguese)

Molina, J.C. (2012), "Study of metallic connections of of wood and concrete composite systems in fire", Post-Doctoral Thesis, São Carlos School of Engineering of the University of São Paulo, São Paulo. (in Portuguese)

Molina, J.C. and Calil Junior, C. (2010), "Development of timber-concrete composite decks in Brazil", *Struct. Eng.*, **88**(5), 26-33.

Molina, J.C., Cheung, A.B. and Calil Junior, C. (2006), "Study of Möhler model in the probability of failure of wood and concrete composite strucutre", *Proceedings of the XXXII Jornadas Sulamericanas de Engenharia Estrutural*, Campinas, Brazil; May. (in Portuguese)

Molina, J.C., Silva, M.A.A.A. and Vasconcelos, R.P. (2015), "Verification of the efficiency of Möhler model in the response of the behavior of wood and concrete composite beams", *Ambiente Construído*, **15**(1), 29-40. http://dx.doi.org/10.1590/S1678-86212015000100004. (in Portuguese)

Monteiro, S.R.S., Dias, A.M.P.G. and Lopes, S.M.R. (2015), "Bi-dimensional numerical modeling of timber-concrete slab-type structures", *Mater. Struct.*, **48**(1), 3391-3406. https://doi.org/10.1617/s11527-014-0407-3.

Pigozzo, J.C., Arroyo, F.N., Christoforo, A.L., Calil Junior, C. and Lahr, F.A.R. (2017), "Pull out strength evaluation of steel bar bonded-in to 45° in round timber of Corymbia citriodora treated with CCA", *Int. J. Mater. Eng.*, **7**(2), 25-32. https://doi.org/10.5923/j.ijme.20170702.02.

Soriano, J. and Mascia, N.T. (2009), "Timber-concrete composite structures: a rational technique for bridges of vicinal roads", *Ciência Rural*, **39**(4), 1260-1269. http://dx.doi.org/10.1590/S0103-84782009005000032. (in Portuguese)

Tomasi, R., Crosatti, A. and Piazza, M. (2010), "Theoretical and experimental analysis of timber-timber joints connected with inclined screws", *Constr. Build. Mater.*, **24**(9), 1560-1571. https://doi.org/10.1016/j.conbuildmat.2010.03.007.

Valipour, H., Khorsandnia, N., Crews, K. and Palermo, A. (2016), "Numerical modelling of timber/timber-concrete composite frames with ductile jointed connection", *Adv. Struct. Eng.*, **19**(2), 299-313. https://doi.org/10.1177/1369433215624600.

Yeoh, D., Fagiacomo, M., Franceschi, M. and Buchanan, K.H. (2011), "Experimental tests of notched and plate connectors for LVL-Concrete composite beams", *J. Struct. Eng.*, **137**(2), 261-269. https://doi.org/10.1061/(ASCE)ST.1943-541X.0000288.

Yttrup, P.J. and Nolan, G. (2001), "Performance of Timber Bridges in Tasmania", http://oak.arch.utas.edu.au, Ago. 28, 2001

HK